BAYESIAN SURROGATES FOR INTEGRATING NUMERICAL, ANALYTICAL AND EXPERIMENTAL DATA: APPLICATION TO INVERSE HEAT TRANSFER IN WEARABLE COMPUTERS

Napoleon Leoni and Cristina Amon
Mechanical Engineering Department and Institute for Complex Engineered Systems
Carnegie Mellon University

ABSTRACT

Wearable computers are portable electronics worn on the body. The increasing thermal challenges facing these compact systems have motivated new cooling strategies such as transient thermal management with thermal storage materials. The ability of building models to quickly assess the effect of different design parameters is critical for effectively incorporating these innovative thermal strategies into new products. System models that enable design space exploration are built from different information sources such as numerical simulations, physical experiments, analytical solutions and heuristics. These models, called surrogates, are nonlinear and adaptive in nature and thus suitable for system responses where limited information is available and few realizations (experiments or numerical simulations) are feasible.

In this paper, the surrogate framework is applied to estimate values for unknown physical parameters of an embedded electronics system. For this purpose, physical experiments and numerical simulations are performed on an embedded electronics prototype system of the TIA (Technical Information Assistant) wearable computer. Numerical models are studied which involve five and three unknown parameters, with and without thermal contact resistances, respectively. Through the use of orthogonal arrays and optimal sampling, an efficient exploration of the parameter space is performed. The objective is to determine system parameters such as thermal conductivities, thermal contact resistances and heat transfer coefficients. Surrogate models are built that combine information obtained from numerical simulations and experimental model measurements as well as from a thermal resistance network simplified model. The integration of several information sources reduces the number of numerical simulations needed to find reliable estimates of the system parameters and allows for identification of the best numerical model. For the embedded electronics case, the use of prior information from the thermal resistance network model reduces significantly the computational effort required to investigate the solution space.

INTRODUCTION

Wearable computers are portable and compact electronic systems that merge information space with user workspace [1]. They are worn on the body [2] and are designed to be lightweight, rugged and power-efficient. Several generations of wearable computers, of increasing complexity, have been designed and manufactured at Carnegie Mellon University (CMU). Figure 1 shows the wearable computer's evolution in terms of the power dissipation per unit area available for heat transfer to the ambient. The exponential increase in the power density together with the complex interactions of a concurrent design process requires innovative design methodologies as well as improved thermal strategies.

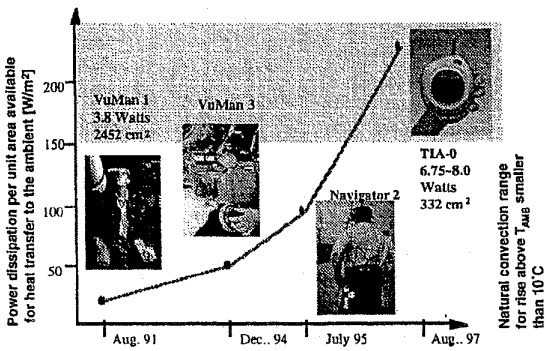

Figure 1: Wearable computer evolution

Wearable computers, and more generally portable electronics, are good examples of how the rising product complexity and the restrictions on time to market introduce a need for shorter design cycles. Simple models and previous experience are commonly used to perform characterization and assessment of different design alternatives in the early stages of a concurrent design process. The possibilities of using more detailed models such as numerical simulations or physical prototypes during these early design stages remain prohibitive due to the large amount of design alternatives that need to be tested. This lack of reliable decision tools -- during conceptual design -- limits many innovative approaches. Paradoxically, these innovative approaches are necessary to attain the sought performance goals.

As an example of how rising product complexity imposes pressures on the development of innovative thermal management strategies, we take a close look at the design requirements imposed on wearable computers. First, we restrict our attention to passive thermal strategies due to battery power limitations. Second, we require a sealed computer housing due to the harsh operation environments. Finally, we need to ensure a reliable operation of the electronics and a safe operation for the user. The latter is attained by keeping the surface of the wearable computer at temperatures below those mandated by ergonomic requirements. The simultaneous

satisfaction of all these constraints is indeed a challenge for the current generation of wearable computers, the TIA (Technical Information Assistant) system. Figure 1 shows that if the TIA's exterior is cooled through free convection only, its steady state housing temperature will rise more than 10°C above ambient, violating the safety operation constraint.

In response to these requirements, we are developing a new manufacturing process that allows for embedding electronic components into polymer substrates [3]. This rapid prototyping process is part of the efforts at the Shape Deposition Manufacturing (SDM) Lab at CMU. The embedding approach offers the advantage of enhanced conduction paths within the system, especially when polymer composites with highly conductive fillers are used [4]. We are also investigating transient thermal management strategies using PCMs (Phase Change Materials) for latent storage [5; 6]. The implementation of PCMs as a stand alone cooling strategy for wearable computers is discussed in Leoni and Amon [7].

From a thermal design viewpoint, to incorporate these cooling technologies into new systems, we have to be able to evaluate their impact early on the product development process. To attain this objective, we need models that capture the effect of different design decisions (variations of the design parameters) on the thermal response of the system and on the satisfaction of the design goals and constraints. Numerical simulations provide a wealth of physical insight into the system behavior but, from the design perspective, they provide only pointwise information (i.e., information for single combinations of the design parameters). On the other hand, performing numerical simulations for a large set of design alternatives would require considerable resources. The challenge is then to gain an understanding of the system behavior through a small number of numerical simulations. The paradigm shift that has been proposed to meet this challenge is to treat numerical simulations as *computer experiments* and build a meta-model (model built from another model) called surrogate which, in spirit, is similar to a response surface or interpolation model of the numerical simulation. The purpose is to replace the numerical simulation with the surrogate during optimization, robustness studies or other design related decision process. In this paper, we present an improvement of this paradigm by building surrogate models that incorporate information not only from numerical simulations but also from knowledge, based on physical principles, that can be synthesized at a lower computational cost than the numerical simulation itself (e.g., approximate analytical solution).

In this paper, we apply our surrogate approach to an inverse heat transfer problem in embedded electronics. First, we present the general formulation of the Bayesian surrogate methodology [8]. Afterwards, we describe the construction of a physical prototype of the embedded electronics system using the SDM process. Thermal measurements are performed on this experimental model using twelve spatially-distributed thermocouples. The objective is to determine, from these temperature measurements, the thermal parameters that govern the system steady state behavior. Thus, the physical parameters to be determined are the conductivity of the polymer used to embed the electronics, thermal contact resistances within the system as well as the heat transfer coefficient representing combined radiation and free convection effects on the external surface of the experimental model. Numerical simulations are performed to model three-dimensional heat conduction within the system using an equivalent heat transfer coefficient for the combined radiation and free convection. Two numerical models for the system are built, which involve three and five unknown parameters, respectively. The numerical model with five parameters considers thermal contact resistances in the system while the other numerical model does not.

We restate our initial objective to find the parameter values that minimize a chosen error measure between the measurements from the experimental model and the predictions from each numerical model considered. We do not try to find these minimizing parameters directly with an optimization procedure. Instead, we build surrogate models for the error measure from a few numerical simulations of different parameter combinations and, then, we use the surrogate model to find the minimizing parameters. One of the surrogate models uses prior information from a first order thermal resistance network in addition to data from the numerical and experimental models. The purpose is to illustrate the possibility of reducing the resources required (i.e., computational effort) to build the surrogate model by using all the available information about the system.

BAYESIAN SURROGATE METHODOLOGY: FRAMEWORK

Surrogate methodologies have been proposed as an alternative to a direct function evaluation of a computationally expensive numerical simulation within an iterative search process (e.g., design optimization). The surrogate approach consists of building an interpolating model that relates the response to the parameters. Then, the computationally inexpensive surrogate substitutes the numerical simulation within the iterative process. Surrogates are meta-models [9] built with information from numerical, experimental or other sources of data. A Bayesian surrogate methodology proposed by Osio and Amon [8] allows for a multi-stage approach to data collection in model building. The Bayesian surrogate methodology integrates the advantages of sampling strategies--aimed to minimize the number of numerical runs or experiments that need to be performed--and a multi-stage approach that allows incremental understanding of the system to be incorporated as the model building process evolves.

The surrogate framework builds upon work on analysis of computer experiments [10]. A detailed mathematical description of the methodology is not included here, and we refer the interested reader to Osio and Amon [8] and Leoni [11]. Only a brief description is provided next.

The surrogate models we implement are based on a regression approach called kriging, which is commonly used in Spatial Statistics [12]. This type of modeling approach does not assume any specific form of the response; instead, models are defined in terms of the correlation between sampling sites and the assumption that the response is a realization of a stochastic process. Sampling sites are parameter combinations

where data has been obtained from any of the information sources. Data collection is performed in stages, and at each stage, a set of correlation parameters is calculated using maximum likelihood estimation with the information gathered at the new sites. The surrogate model is updated at each stage using the surrogate of the previous stage as a prior distribution, such that we use all the information that has been gathered up to the current stage. Information known about the system can be incorporated in the form of a prior distribution for the first stage of data collection. If this prior information comes from a physical model of the system, we call it a physical prior.

Sampling strategies (i.e., selection of the sampling points where information is gathered at each stage) are critical to achieve the desired accuracy of the surrogate model while keeping the number of sampling points to a minimum. For the first stage of data collection, we use maximin orthogonal arrays and latin hypercubes [13; 14] which have good projection properties as well as uniform coverage of the design space. These are especially suitable for an initial stage when very little information is available about the variation of the response within the design space. Optimal sampling [10] provides advantages for subsequent stages of data collection because it selects where the next set of runs has to be performed based on the information gathered up to the current stage. Optimal sampling is implemented such that the selected sites minimize the predictive error for the following stage.

In summary, the surrogate approach consists of building a model based on information of a discrete set of data, with the underlying hypothesis that obtaining this information requires a considerable amount of resources (e.g., time, computation, etc.). Other approaches could substitute the kriging model building approach, such as Artificial Neural Networks or the model building process based on Response Surface Methodologies [15]. Artificial Neural Networks (ANN) provide a general framework for building reliable interpolating models. However, the application of ANN generally requires a large number of observations (e.g., numerical simulations or experiments) to calibrate their response [16]. Under our assumption that the numerical simulations require a considerable amount of resources, the ANN approach would prove less efficient. Response Surface Methodology (RSM) has been also used extensively in building models for the outcomes of physical experiments. It has the characteristic of requiring a priori assumption about the form of the response (i.e., linear or quadratic). Also, traditional RSM places major emphasis on the reduction of the model uncertainty due to random error, while we are more concerned about the systematic bias of the model from the actual response. An additional advantage of the surrogate modeling methodology we propose is that, through the use of different sources of information, we gain as a feedback an improved physical insight and a potentially reusable knowledge instead of just a numerical black box.

EMBEDDED ELECTRONICS SYSTEM: Description and Experimental Setup

The geometry of the embedded electronics system selected for the study, shown in Fig. 2, resembles a simplified version of the TIA wearable computer. The experimental model is manufactured with SDM [3] by successively depositing polymer layers. The system is comprised by a polymer substrate (black substrate) and by an external rubber harness (white strip) that partially covers the sides of the substrate.

The polymer substrate is made of epoxy stycast 2651 MN (Grace Specialty Polymers) and consists of four layers of deposited material, as depicted in Fig. 3. Between the second and third epoxy layers, a heat generating component and an aluminum heat spreader are embedded into the substrate. The heat generating component is a strip heater from OMEGA and it is used in substitution of the complex electronics included in the TIA. The heat spreader is a 1/16" thick aluminum plate, placed on the top of the strip heater as shown on the experimental model cross section of Fig. 3.

The three basic steps for building the experimental model through SDM are: deposition, machining and embedding. The deposition step involves pouring the epoxy into the mold until the desired layer thickness is achieved. After the epoxy has cured, machining is performed to attain the desired layer shape. The purpose of the machining step could involve: achieving a flat face, machining pockets to embed a specific electronic component or shaping a curved surface. In our experimental model, a shallow pocket was machined to allow for the strip heater to level with the remaining epoxy layer.

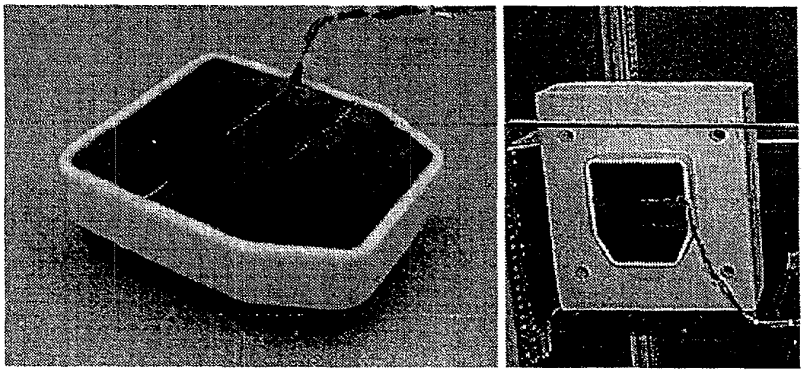

Figure 2: SDM Experimental model of TIA Wearable Computer (left) and Experimental Setup (right)

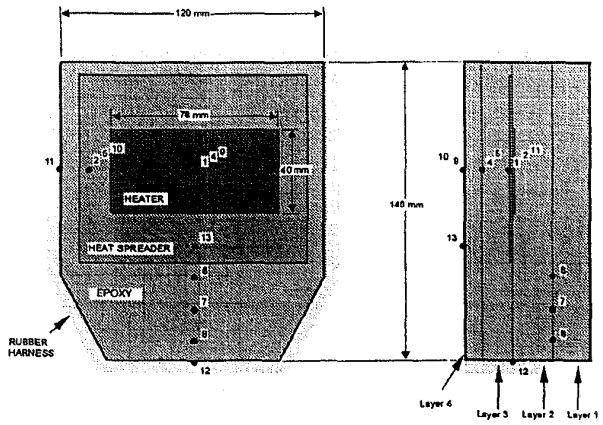

Figure 3: Experimental model cross section

The embedding step consists of placing and attaching the components and sensors within the system. The thermocouples are held in place by bonding them to the epoxy with an adhesive (Omegabond 100). The heater is bonded first to the aluminum heat spreader and, then, both are bonded to the epoxy layer using the Omegabond adhesive. The physical boundaries of each layer are shown with dotted lines in Fig. 3. Notice that several thermal contact resistances could arise because of the manufacturing process used. We call interlayer thermal contact resistance the one between any two neighboring layers of epoxy. This contact resistance may be due to entrapped gases between the two layers during manufacturing. A thermal contact resistance could arise as well between the aluminum heat spreader and the epoxy layer deposited on top of it (Layer 3 in Fig. 3). We refer to this as the aluminum/epoxy thermal contact resistance.

Thirteen K-type Omega thermocouples are embedded in the experimental model, and their locations are shown in Fig. 3. Thermocouple labels that point to the same location in the different views of Fig. 3 represent the condition of several thermocouples lying colinearly in that view. Thermocouple #3 was not used for this base case experimental model and thus it will be omitted from subsequent discussions. The thermocouple signals are recorded and converted to temperature measurements using a DT-2801 board and PC-Lab software for data acquisition, both from Data Translation. Sampling of the transient temperatures is done every 2 minutes for a total time of 8 hours. Four different power dissipation levels at the heater are used to perform measurements: 5, 6.75, 8 and 10 Watts. The power level is determined from the known resistance of the strip heater and a controlled current generated with a regulable power source. In this paper, we illustrate the analyses using the steady state results for the 8 Watt power level. The experimental setup is shown in Fig. 2. The embedded system is positioned vertically with its back and the portion of its sides not covered by the rubber harness, placed into a pocket of a styrofoam block in order to insulate this portion of the boundary. A thorough explanation of how the experimental model is built and how the measurements are performed is presented in Prodan and Amon [17].

The results for the average steady state temperatures at each of the thermocouples are shown in Table 1. This table also shows error estimates for the experimental temperature measurements. We perform an uncertainty analysis as outlined by Moffat [18] to make error estimates. These estimates represent a 95% confidence region based on the variance of the experimental measurements. The experimental error estimates include a random component present during the ice bath calibration of the thermocouples as well as a scatter component registered during the actual experiment, which is due to variations in the room conditions while the experiment was performed.

Table 1: Experimental measurements and error estimates

Thermo-couple	T_i^{EXP} [°C]	δT_i^{EXP} [°C]
1	42.9	0.3
2	40.5	0.3
4	32.8	0.3
5	30.0	0.3
6	29.7	0.2
7	24.6	0.2
8	20.3	0.2
9	28.0	0.3
10	22.6	0.4
11	29.8	0.3
12	14.3	0.3
13	24.5	0.3

NUMERICAL MODELING

Our objective is to identify a numerical model and a set of physical parameters which, when combined, can reliably predict the behavior of the system. With this objective, we consider two numerical models that might capture the physical behavior of the system. We obtain the spatial temperature distribution for both numerical models by solving the steady state heat conduction problem, using a spectral element method [19; 20] within the three dimensional domain of the system. Both numerical models preserve the geometry of the system as built in the experimental model, and a symmetry condition is used to reduce the computational domain by half. Two types of boundary conditions are used in these numerical models. The portion of the system surface which is surrounded with styrofoam panels in the experimental model (Fig. 2b) is specified as an insulated boundary. The remaining surface of the system, which includes the rubber harness surface and the epoxy substrate surface, are specified with a single, uniform heat transfer coefficient (U_{AMB}) representing combined radiation and free convection to the ambient.

The two different numerical models are described in Table 2. Numerical Model No. 1 (NM1) involves three unknown parameters, which are the conductivities of the epoxy and the rubber harness (assumed to be uniform throughout the domain) and the heat transfer coefficient. The ranges for these parameters

are chosen according to our physical insight of the problem and are reported in Table 2. Numerical Model No. 2 (NM2) includes two more parameters in addition to those of NM1, which represent effective conductivities to quantify two thermal contact resistances that might arise in the system. To model numerically the contact resistances, we introduce a thin layer of material in the computational domain with a conductivity k_{IR} or $k_{AL/E}$. The thickness (t_{LAYER}) of this layer in the numerical model is chosen such that we can consider the heat transfer in that layer to be essentially one dimensional.

The one dimensional thermal resistance of the layer can be expressed as a function of the conductivity assigned to it in the numerical model. The equivalent thermal resistance associated with this layer represents two thermal resistances in parallel: one due to the contact resistance and the other due to conduction through an epoxy layer of thickness t_{LAYER}:

$$R_{T,LAYER} = t_{LAYER} / k_{LAYER} = R_{T,C} + t_{LAYER} / k_{EPOXY} \Rightarrow$$
$$R_{T,C} = t_{LAYER} / k_{LAYER} - t_{LAYER} / k_{EPOXY}$$

where k_{LAYER} represents either k_{IR} or $k_{AL/E}$, $R_{T,C}$ is the thermal contact resistance present in the system and $R_{T,LAYER}$ represents the total thermal resistance assigned to that material layer which physically is always positive. Expressing $R_{T,LAYER}$ as a function of the layer conductivity and the epoxy conductivity, then both k_{IR} and $k_{AL/E}$ have to be less or equal than k_{EPOXY}. In expressing the ranges for k_{IR} and $k_{AL/E}$ in Table 2, we also indicate in brackets the actual ranges for the thermal contact resistance ($R_{T,C}$). To assess the performance of these two numerical models, we need to address the following questions:

- Which is an appropriate value for the conductivity of the epoxy in our experimental SDM prototype?
- Is it important to consider thermal contact resistances in modeling the system? If so, how do we quantify them?
- Is it a good assumption to consider a uniform heat transfer coefficient (due to natural convection and radiation) on the wearable computer surface?

To answer these questions, we would like to require the minimum number of numerical simulations and experimental measurements because of the expense in resources they represent. To achieve this objective, we use the surrogate methodology.

Application of Surrogate Framework to Inverse Heat Transfer Problem

Inverse Heat Conduction Problems (IHCP) have been studied extensively in the past. Researchers have uncovered a set of difficulties when solving these kinds of problems: ill-posedness, solutions very sensitive to changes in input data and possible non-uniqueness of the solutions. The IHCP consists of retrieving the most accurate values for a set of unknown system parameters by minimizing the discrepancy between a proposed model for the system and measurements taken from a physical prototype of the system.

Jarny et al. [21] proposed an adjoint equation method for solving the general multidimensional IHCP. Their approach offers a framework where the minimization of a functional allows for the determination of values for the unknown parameters. Implementation of their approach requires solving the adjoint problem, which is of similar complexity to the original heat transfer problem, for each iteration of the optimization procedure. Beck [22] compared the relative performance of the two most used approaches for the inverse problem: the Function Specification and the Iterative Regularization methods. As system complexity rises, analytical solutions might be unfeasible, and numerical approaches become necessary for building numerical models.

Table 2: Numerical Models

Model No.	Modeling Assumptions	Output	Model Parameters	Design Space
1	Uniform epoxy and rubber conductivities, uniform external heat transfer coefficient	Temperature distribution	k_{EPOXY} U_{AMB} k_{RUBBER}	0.3-0.7 W/m °C 8-15 W/m² °C 0.1-1.0 W/m °C
2	Uniform epoxy and rubber conductivities, uniform external heat transfer coefficient, uniform and equal thermal contact resistance between epoxy layers, and uniform contact resistance between aluminum heat spreader and epoxy; t_{LAYER} = 0.04 cm	Temperature distribution	k_{EPOXY} U_{AMB} $k_{IR}[R_{T,C:IR}]$ ...models interlayer contact resistance $k_{AL/E}[R_{T,C:AL/E}]$ ...models contact resistance for aluminum & epoxy interface k_{RUBBER}	0.4-0.7 W/m °C 10-13 W/m² °C 0.01[343]-0.7[0.0] W/m°C [°C cm²/W] $k_{IR} \leq k_{EPOXY}$ 0.1[34.3]-0.7[0.0] W/m°C [°C cm²/W] $k_{AL/E} \leq k_{EPOXY}$ 0.1-1.0 W/m °C

Osman et al. [23] shows a general approach to the two dimensional IHCP in which a finite element analysis code is embedded within the optimization procedure for determining the values of the sought parameters.

A common feature to all this work is the availability of a system analytical or numerical model that can be used intensively within an optimization procedure. However, many engineering problems require numerical models for which a single numerical simulation is already computationally demanding, let alone an iterative procedure with hundreds of calls. For this level of complexity, we require a different approach in which we do not deplete the resources available for solving the problem before we reach a satisfactory solution. In this paper, we focus on this next level of complexity and evaluate how our surrogate approach can reduce the amount of resources used to solve problems that fall into this classification.

To incorporate the surrogate framework into the inverse problem of determining a set of unknown parameters by comparing a benchmark model of the system (e.g., experimental model) with a model that needs to be tuned with those parameters (e.g., numerical model), we propose the general procedure presented below. At each step of the procedure, we also indicate the particular decisions we have to make concerning the example illustrated in this paper:

1. *Select a benchmark model and a set of state variables as reference values.* We use the experimental model presented before and twelve temperatures measured at different spatial locations as reference values for the state variables.
2. *Choose a numerical model to be tuned with a set of unknown physical parameters, called design parameters.* We select the two numerical models NM1 and NM2 with their respective parameters.
3. *Define initial ranges and constraints for the unknown parameters and propose a sampling strategy where each sampling site represents a run of the numerical model with a different combination of values for the design parameters.* The initial ranges and constraints for our design parameters are presented in Table 2. As sampling strategies, we use orthogonal arrays which are introduced later in Table 3.
4. *Choose a quantitative measure, involving the state variables, for the error in the numerical simulation predictions as compared to the benchmark model. Build a surrogate model that approximates the behavior of this error as a function of the design parameters.* We choose the e_{RMSE} (Root Mean Squared Error) as a metric for comparison between the numerical simulations and the experiments. The e_{RMSE} is defined as:

$$e_{RMSE} = \sqrt{\frac{1}{N} \cdot \sum_{i}^{N} (T_i^{NS} - T_i^{EXP})} \qquad (1)$$

where the subscript i runs over all the thermocouples where experimental data is available (i = 1,..,N; N=12).

5. *Minimize the surrogate model for the error measure to obtain estimates of the minimizing values for the unknown parameters. At this step, a procedure such as the Iterative Regularization Method could be incorporated to ensure that the optimization procedure selects a set of physically viable values for the parameters.* We denote with $\hat{e}_{RMSE}$ the same error metric as defined by (1) with T_i^{NS} substituted by $\hat{T}_i^{NS}$ which is the surrogate approximation to the numerical temperature. We minimize the $\hat{e}_{RMSE}$ using a simplex simulated annealing algorithm.
6. *Verify the accuracy of the surrogate model at the minimizing parameter values with an additional numerical simulation. If the results are not satisfactory, two main actions could be taken: (a) improve the surrogate model by gathering more information, go to step #2 but use a reduced subset of the original parameters space, or (b) choose a different numerical model and restart from step #1.*

Our goal in following the above-described procedure is to identify a numerical model that is experimentally validated so that it can be reliably used for testing different design alternatives and operating conditions. The objective of following this incremental approach is to find the numerical model of lowest complexity that provides the desired accuracy.

Since we will evaluate two different numerical models and there are several alternatives when building the surrogate models, we illustrate the approach by studying three different cases of surrogate models and evaluating their performance. Table 3 presents a description of the different cases of surrogate models to be studied. Note that for Cases I and II, we use a non informative prior distribution. This non informative prior - constant throughout the design space- is the average value of the response estimated from the information obtained by running the numerical simulations.

For each surrogate model, we indicate in Table 3 the type of sampling strategy to select the sites where numerical simulations are performed. Surrogate model I involves three unknowns and thus implies a three dimensional search space. As the complexity of the numerical model is increased, the number of unknown parameters also increases, thus surrogate models II and III involve a five dimensional search space.

To attain the same degree of accuracy of Case I for the five dimensional design space of Case II, we need roughly the square (5/3 power) of the number of sampling points, assuming the complexity of the effects for each parameter to be the same. However, due to the computational cost of running ~$(16)^2$ numerical simulations, we stopped gathering data after two stages of 25 sampling points each.

Table 3: Cases for surrogate models

Case	Numerical Model	Experimental Design	No. of runs	Response modeled	Prior Distribution
I	1	1st stage: 16 run orthogonal array	16	Surrogates built for each of the 12 temperatures; $\hat{e}_{RMSE}$ built from these surrogates	Constant
II	2	1st stage: 25 run latin hypercube; 2nd stage: 25 run optimal sampling	50	Surrogates built for each of the 12 temperatures; $\hat{e}_{RMSE}$ built from these surrogates	Constant
III	2	1st stage: 25 run latin hypercube	25	Surrogates built for each of the 12 temperatures; $\hat{e}_{RMSE}$ built from these surrogates	Thermal resistance network model

Case III is an interesting example which incorporates our physical understanding of the system in the form of a prior distribution, with the objective of reducing the required number of numerical simulations. For the three dimensional heat conduction problem a relatively simple physical model for the temperatures is a Thermal Resistance Network (TRN). This physical model is built by solving a resistance network that emulates the heat conduction paths within the system. The result is an analytical expression yielding the temperatures that we are modeling as a function of the five design parameters ($T_i^{TRN}[k_{EPOXY}, U_{AMB}, k_{IR}, k_{AL/E}, k_{RUBBER}]$). This resistance network yields a qualitatively correct model for the effects due to each of the variables; however, it is too crude to be used directly as a prior, so instead we use the following physical prior:

$$T_i^{PRIOR} = \beta_1 + \beta_2 * T_i^{TRN}[k_{EPOXY}, U_{AMB}, k_{IR}, k_{AL/E}, k_{RUBBER}] \quad \text{for } i = 1,..,12$$

which is a linear combination of the thermal resistance network prediction. The values for the statistical parameters β_1 and β_2 are obtained from a generalized least squares fitting to the information gathered from the numerical simulations.

As Table 3 shows, we build surrogate models for the temperatures predicted by the numerical model; in other words, for each T_i^{NS}, we build a surrogate model that approximates its behavior $\hat{T}_i^{NS}$ as a function of the design parameters. Afterwards, using the measurements from the experimental model (T_i^{EXP}), we construct the $\hat{e}_{RMSE}$ function which is a surrogate model of the true e_{RMSE}. We build surrogates for the temperatures instead of directly building surrogates for the error function because this allows us to incorporate prior knowledge based on our physical understanding of the relationship between the temperatures and the design parameters.

DISCUSSION

Once the surrogate models are built, we can optimize them to find the minimizing parameter values, we can compare their predictions with new numerical simulations at untested sites in order to test their predictive reliability, and we can also visualize them to gain physical insight about the responses.

If we optimize numerically the surrogate models ($\hat{e}_{RMSE}$) for each of the cases considered, we obtain estimates of the minimizing parameters for the e_{RMSE} metric. The results from this minimization are shown in Table 4, where * represents the minimizing parameter values.

Table 4: Minimizing parameters for $\hat{e}_{RMSE}$

Case	$\hat{e}_{RMSE}$	k^*_{EPOXY}	U^*_{AMB}	k^*_{RUBBER}	k^*_{IR}	$k^*_{AL/E}$
I	0.71	0.48	11.1	0.66	-	-
II	0.67	0.50	11.8	0.46	0.044	0.50
III	0.60	0.47	11.1	0.72	0.19	0.47

Table 4 shows that the three surrogate models predict similar values for the conductivity of the epoxy (within 4%) as well as for the heat transfer coefficient values (within 6%). Physically, the error metric e_{RMSE} has units of degrees centigrade and the surrogates predict average temperature differences between the numerical model and the experimental model of about 0.7°C for NM1 (from surrogate I) and between 0.6°C and 0.7°C for NM2 (from surrogate models II and III). Another interesting result is that both surrogate cases II and III predict that the best numerical model would be one in which there is no contact resistance between the aluminum heat spreader and the epoxy ($k^*_{EPOXY}=k^*_{AL/E}$). The major discrepancies between the different surrogate model minimizing predictions arise in the values for the k_{RUBBER} and k_{IR}. Still, both Cases II and III predict that there is an interlayer thermal contact resistance.

Substituting these minimizing parameters into the corresponding numerical model, we run simulations and compare their results with the surrogate predictions to assess the accuracy of the surrogates in predicting the e_{RMSE} and the temperatures. Table 5 shows, for each of the three cases, the difference between the surrogate model and the numerical model predictions for each temperature. In general, all surrogate predictions are within 1°C of the numerical model results. The largest errors are registered for Case II, even though this surrogate model employs twice as many numerical simulations as those used to build the surrogate model for Case III. This result indicates the advantage of incorporating the additional information given by the thermal resistance network physical

prior. Even more interesting is the fact that, at the optimal parameter settings, the surrogate model from Case III outperforms in predictive capability the surrogate from Case I. The latter is remarkable given the higher dimensionality of the search space for Case III (5 vs. 3 dimensions) as compared to the relatively small increase in the number of observations used to build the surrogate model (only 25 as compared to 16).

Table 5: Surrogate prediction error at minimizing parameters

	$\|\hat{T}_i^{NS}-T_i^{NS}\|$ [°C]		
	Case I	Case II	Case III
1	0.59	0.23	0.06
2	0.60	0.08	0.10
4	0.40	0.86	0.12
5	0.35	0.41	0.16
6	0.50	0.63	0.14
7	0.37	0.43	0.05
8	0.12	0.77	0.13
9	0.20	0.98	0.14
10	0.03	1.17	0.25
11	0.23	0.74	0.67
12	0.06	0.04	0.47
13	0.03	1.20	0.19

The numerical model temperature predictions for the set of minimizing parameters obtained from optimizing the $\hat{e}_{RMSE}$ are shown in Table 6. In this Table, we also show the absolute error of the numerical predictions as compared to the experimental measurements and the corresponding e_{RMSE}.

From Table 6, we can rank the different surrogate cases in order of decreasing performance of their minimizing parameters as: Case III, Case I and Case II with e_{RMSE} of 0.71, 0.81 and 1.02, respectively. In terms of how close the surrogate prediction ($\hat{e}_{RMSE}$) is to the actual error (e_{RMSE}), surrogate case I predicts an error within 12%, surrogate case III within 15% and surrogate case II within 30%. The numerical model temperature predictions at the corresponding minimizing parameters obtained from surrogate models I and III yield similar absolute errors when compared to the experimental model measurements. These absolute errors are on the order of 0.2 to 0.7 °C for all of the thermocouples, except for T_5^{NS} (i.e., location 5 in Fig. 3) that differs by almost 2 °C from the experimental measurement.

To discuss the existence of thermal contact resistances, we visualize the surrogate responses. Since the surrogate models are multidimensional, we only visualize two parameters at a time while keeping the other parameters fixed. In the following figures, all the parameters that are not included in the axes are kept fixed at the minimizing values of that surrogate model case. Figure 4 shows the surrogate model case I as a function of k_{EPOXY} and U_{AMB}. The plot shows a clear minimum for the $\hat{e}_{RMSE}$ in the interior of the domain, which is the value reported in Table 4. Figure 4 also shows that the $\hat{e}_{RMSE}$ value is relatively sensitive to changes in both k_{EPOXY} and U_{AMB}. This implies that we can identify a small region where we can assure that the minimizing parameter values are contained with a confidence degree limited by the experimental uncertainty in the temperature measurements.

Table 6: e_{RMSE} for numerical model at minimizing parameters from surrogate

Physical location		Case I		Case II		Case III	
[i]	T_i^{EXP}[°C]	T_i^{NS}[°C]	$\|T_i^{NS}-T_i^{EXP}\|$	T_i^{NS}[°C]	$\|T_i^{NS}-T_i^{EXP}\|$	T_i^{NS}[°C]	$\|T_i^{NS}-T_i^{EXP}\|$
1	42.9	42.1	0.8	42.8	0.1	42.6	0.3
2	40.5	39.7	0.8	40.4	0.0	40.2	0.2
4	32.8	32.6	0.2	33.6	0.8	33.0	0.2
5	30.1	28.0	2.0	28.9	1.2	28.4	1.7
6	29.7	30.0	0.4	30.7	1.1	30.3	0.6
7	24.6	24.8	0.2	25.7	1.1	25.0	0.4
8	20.3	20.9	0.6	21.9	1.5	21.0	0.6
9	28.0	27.8	0.2	26.2	1.8	27.8	0.2
10	22.6	23.6	1.1	22.1	0.5	23.6	1.0
11	29.9	29.2	0.6	30.1	0.2	29.2	0.7
12	14.3	13.7	0.6	14.1	0.1	13.6	0.7
13	24.5	24.6	0.1	23.1	1.4	24.6	0.1
e_{RMSE}			0.81		1.02		0.71

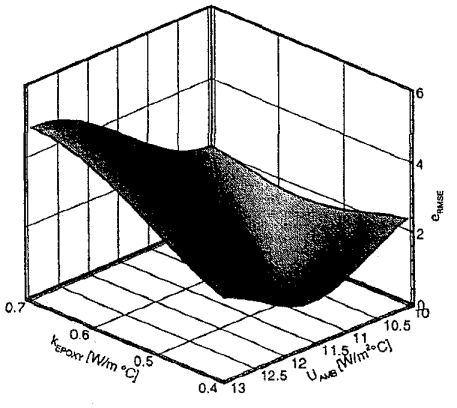

Figure 4: $\hat{e}_{RMSE}$ from surrogate model case I

Figure 5 shows the $\hat{e}_{RMSE}$ surrogate as a function of k_{EPOXY} and k_{IR}. The surface is bounded with two planes that represent the constraints in the parameter space indicated in Table 2 and depicted in Fig. 5. This figure shows that the surrogate model II predicts a relatively small variation for the error throughout the k_{EPOXY} and k_{IR} space, as $\hat{e}_{RMSE}$ is bounded between 0.6 and 2.0. The minimum values for $\hat{e}_{RMSE}$ lie in the lower bound for k_{IR} and, in this region, the response is very unsensitive to changes in k_{EPOXY} yielding a smaller confidence in the minimizing value k^*_{EPOXY} even though its magnitude is similar to the other surrogate model predictions. Also, as an indicator of the surrogate model case II reliability, at the minimizing values it underpredicts by 30% the actual e_{RMSE} from the numerical model shown in Table 6.

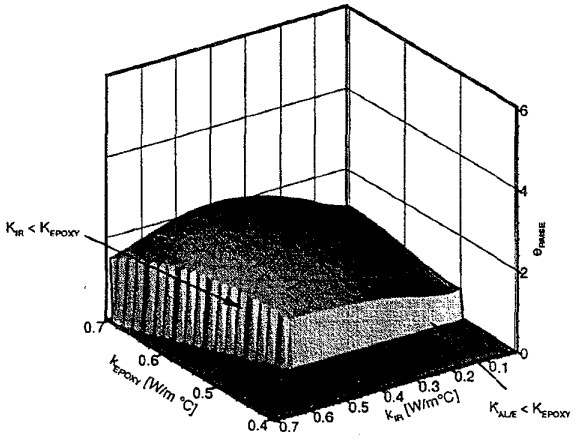

Figure 5: $\hat{e}_{RMSE}$ from surrogate model case II

The surface plot for the $\hat{e}_{RMSE}$ from surrogate model III is shown in Fig. 6. This surrogate model predicts a high sensitivity of the error with respect to the parameter k_{EPOXY}. Therefore, for the minimizing value predicted of $k^*_{AL/E}$, we have a high confidence in the determination of the epoxy conductivity. Also, in the considered range for k_{EPOXY}, the dependence of $\hat{e}_{RMSE}$ on this parameter is almost linear. Nonlinearities do appear in the response variation with the parameter k_{IR}, for which the surrogate predicts a zone of relative insensitivity to the parameter and then a sharp rise of the error when the value drops below a certain threshold. Notice the difference between this sort of response and the one predicted from surrogate model II.

Even though surrogate model III predicts the minimizing value for the k_{IR} parameter to be closer to its lower bound than to its upper bound, the relative insensitivity of $\hat{e}_{RMSE}$ with respect to k_{IR} and the fact that the surrogate is just an approximation to the e_{RMSE} function, motivates us to inquire more closely about the behavior of the e_{RMSE} in this region. Formally, we would need to update the surrogate model III with a new set of observations gathered in a progressively smaller region of the parameter space (i.e., similar to bracketing the minimum) until obtaining a subset of the original space small enough to use the direct insertion approach (i.e., optimization with a direct call to the numerical simulations).

For the purpose of illustration in this paper, we perform two additional numerical simulations, keeping all the parameters fixed to the minimizing values obtained from surrogate model III but assigning to k_{IR} its upper bound (k_{IR}= k^*_{EPOXY} = 0.47 W/m °C) and its lower bound (0.01 W/m °C). The results obtained for the e_{RMSE} are 0.80 for the upper bound (i.e., no interlayer thermal contact resistance) and 4.42 for the lower bound of k_{IR}. These results confirm the behavior of the surrogate model III which predicts the minimum for the e_{RMSE} to correspond to a numerical model with non zero interlayer thermal contact resistance. However, as the difference between the temperature predictions at the higher bound for k_{IR} and at the minimizing value k^*_{IR} is on the order of the experimental error, this implies that, using the available experimental information, we could not infer with certainty whether there is an interlayer thermal contact resistance.

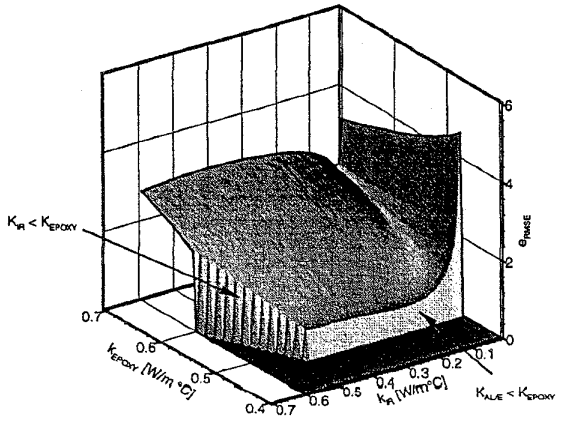

Figure 6: $\hat{e}_{RMSE}$ from surrogate model case III

A physical explanation of the insensitivity of the error measure to the k_{IR} parameter can be given observing the spatial layout of the thermocouples in Fig. 3. Due to the manufacturing process itself, we could only embed thermocouples in the epoxy layer interfaces. When both k_{EPOXY} and k_{IR} are varied, these thermocouples only sense a change in the effective conductivity of the whole layer. Thus, if there is a

set of pairs k_{EPOXY} and k_{IR} yielding the same effective conductivity, then these embedded thermocouples will only reflect slight changes.

CONCLUSIONS

This paper illustrates the use of the Bayesian surrogate methodology to determine a set of unknown physical parameters and to select the most suitable numerical model for an embedded electronics system based on experimental information. We show the potential of using this methodology to reduce the burden of solving inverse heat transfer problems when computationally-expensive numerical simulations are required. Two numerical models for the embedded electronics system were investigated with three and five unknown parameters which correspond to neglecting and accounting for contact resistance, respectively. Surrogate models are built for an error metric which compares the numerical model predictions to the experimental model measurements. By minimizing these surrogates, we estimate the values of the unknown physical parameters.

The application of the surrogate methodology to the inverse heat transfer problem provides a framework to enhance the integration of different information sources into the model building process. The advantage of this integration is that none of the information available about the system is neglected when building a model, which reduces the amount of information required from resource intensive sources such as detailed numerical simulations.

Our study reveals that incorporating prior information from a thermal resistance network reduces by at least a factor of two the numerical simulations required to make reliable inferences about the set of unknown physical parameters. The predicted values for the conductivity of the epoxy are within 4% for all the surrogates built from the two different numerical models. However, the surrogate model with prior information requires the least number of numerical simulations to yield this prediction, in the case of the numerical model accounting for thermal contact resistances. Also, the confidence in the epoxy conductivity estimate from the surrogate with the prior information is greater because it predicts a higher sensitivity of the error metric with respect to this parameter. It is not possible to infer whether there is a thermal contact resistance between layers of deposited material. The numerical models chosen perform well in predicting the experimental model measurements. In fact, the numerical model with five parameters agrees with the measurements from the experimental model with an error on the order of the experimental uncertainty for all but one of the twelve thermocouple measurements.

ACKNOWLEDGMENTS

The authors gratefully acknowledge the support of the National Science Foundation Grant CTS-9630801, the Advanced Research Project Agency Grant DABT 63-95-C-0026 and the Program *Beca Credito* of CONICIT.

REFERENCES

[1] Smailagic, A. and Siewiorek, D.P., "Interacting with CMU Mobile Computers," *IEEE Personal Communication*, Vol. 3, No. 1, pp. 6-16, 1996.

[2] Amon, C.H., Nigen, J.S., Siewiorek, D.P., Smailagic, A., and Stivoric, J.M., "Concurrent Design and Analysis of the Navigator Wearable Computer System: The Thermal Perspective," *IEEE Transactions on Components, Packaging, and Manufacturing Technology*, Vol. 18, No. 3, pp. 567-577, 1995.

[3] Finger, S., Stivoric, J.M., Amon, C.H., Gursoz, L., Prinz, F., Siewiorek, D., Smailagic, A., Weiss, L., "Reflections on a Concurrent Design Methodology: A Case Study in Wearable Computer Design," *Computer-Aided Design*, Vol. 28, No. 5, pp. 393-404, 1996.

[4] Egan, E. and Amon, C.H., "Thermal Design of Wearable Computers: Application to the Navigator2, Thermal Management Devices, and Embedded Electronics," EDRC Report No. 24-123-95, Carnegie Mellon University, Pittsburgh, Pennsylvania, 1995.

[5] Pal, D., and Joshi, Y.K., "Application of Phase Change Materials to Thermal Control of Electronic Modules: A Computational Study," *ASME Advances in Electronic Packaging*, Vol. 10, No. 2, pp. 1307-1316, 1995.

[6] Estes, R.C., "The Effect of Thermal Capacitance and Phase Change on Outside Plant Electronic Enclosures," *IEEE Transactions on Comp., Hybrids, and Manufacturing Technology*, Vol. 15, No. 5, pp. 843-849, 1992.

[7] Leoni, N., and Amon, C.H., "Thermal Design for Transient Operation of the TIA Wearable Portable Computer," *Proceedings of the ASME INTERpack '97 Conference*, Hawaii, June 15-18, pp. 2151-2161, 1997.

[8] Osio, I.G. and Amon, C.H., "An Engineering Design Methodology with Multistage Bayesian Surrogates and Optimal Sampling," *Research in Engineering Design*, Vol. 8, pp. 189-206, 1996.

[9] Yesilyurt, S., Ghaddar, C., Cruz, M. and Patera A.T., "Bayesian-Validated Surrogates for Noisy Computer Simulations; Application to Random Media," *SIAM Journal on Scientific Computing*, 1993.

[10] Sacks, J., Welch, W.J., Mitchell, T.J. and Wynn, H.P., "Design and Analysis of Computer Experiments," *Statistical Sciences*, Vol. 4, No. 4, pp 409-435, 1989.

[11] Leoni, N., Ph.D. Thesis, Department of Mechanical Engineering, Carnegie Mellon University, Pittsburgh, PA, in progress.

[12] Cressie, N., *Statistics for Spatial Data*, John Wiley and Sons, 1991.

[13] Owen, A., "Orthogonal Arrays for Computer Experiments Integration and Visualization," *Statistica Sinica*, Vol. 2, pp 439-452, 1992.

[14] Osio, I.G., Ph.D. Thesis, Department of Mechanical Engineering, Carnegie Mellon University, Pittsburgh, PA, 1996.

[15] Myers, R.H., and Montgomery, D.C., *Response Surface Methodology: Process and Product Optimization Using Designed Experiments*, John Wiley and Sons, 1995.

[16] Cheng, B., and Titterington, D.M., "Neural Networks: A Review from a Statistical Perspective," *Statistical Science*, Vol. 9, No. 1, pp 2-30, 1994.

[17] Prodan, T., M.S. Thesis, Department of Mechanical Engineering, Carnegie Mellon University, Pittsburgh, PA, 1998.

[18] Moffat, R.J., "Uncertainty Analysis," in *Thermal Measurements in Electronics Cooling*, edited by Kaveh Azar, CRC Press, pp 45-81, 1997.

[19] Patera, A.T., "A Spectral Element Method for Fluid Dynamics: Laminar Flow in a Channel Expansion," *Journal of Computational Physics*, Vol. 54, pp. 468-477, 1984.

[20] Amon, C.H., "Spectral Element-Fourier Method for Unsteady Conjugate Heat Transfer in Complex Geometry Flows," *AIAA J. Thermophysics and Heat Transfer*, Vol. 9, No. 2, pp. 247-253, 1995.

[21] Jarny, Y., Ozisik, N. and Bardon, J.P., "A general optimization method using adjoint equations for solving multidimensional inverse heat conduction," *International Journal of Heat and Mass Transfer*, Vol. 34, No. 11, pp. 2911-2919, 1991.

[22] Beck, J.V., "Comparison of the iterative regularization and function specification algorithms for the inverse heat conduction problem," *ASME First Conference in a Series on Inverse Problems in Engineering*, Palm Coast, Florida, June 13-18, 1993.

[23] Osman, A.M., Dowding, K.J., and Beck, J. V., "Numerical Solution of the General Two-Dimensional Inverse Heat Conduction Problem (IHCP)," *ASME Journal of Heat Transfer*, Vol. 119, No. 38, 1997.